Analytica Chimica Acta 770 (2013) 7–17

Contents lists available at SciVerse ScienceDirect

Analytica Chimica Acta

journal homepage: www.elsevier.com/locate/aca

Optimization of chemical and instrumental parameters in hydride generation laser-induced breakdown spectrometry for the determination of arsenic, antimony, lead and germanium in aqueous samples

Semira Ünal Yeşiller, Şerife Yalçın*

İzmir Institute of Technology, Faculty of Science, Chemistry Department, 35430 Urla, İzmir, Turkey

HIGHLIGHTS

- Continuous flow hydride generation technique for LIBS detection of As, Sb, Pb and Ge.
- Optimization of chemical and instrumental parameters in HG-LIBS.
- Quantitative determination of As, Sb, Pb and Ge in aqueous samples.
- Enhancements in LOD values compared to direct liquids analysis by LIBS.
- Investigation of the effect of carrier gas on LIBS signal strength.

GRAPHICAL ABSTRACT

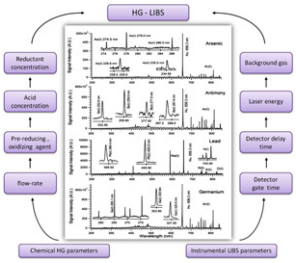

ARTICLE INFO

Article history:
Received 20 November 2012
Received in revised form 4 February 2013
Accepted 7 February 2013
Available online 16 February 2013

Keywords:
Laser-induced breakdown spectroscopy
Hydride generation
Toxic elements
Detection limit

ABSTRACT

A laser induced breakdown spectrometry hyphenated with on-line continuous flow hydride generation sample introduction system, HG-LIBS, has been used for the determination of arsenic, antimony, lead and germanium in aqueous environments. Optimum chemical and instrumental parameters governing chemical hydride generation, laser plasma formation and detection were investigated for each element under argon and nitrogen atmosphere. Arsenic, antimony and germanium have presented strong enhancement in signal strength under argon atmosphere while lead has shown no sensitivity to ambient gas type. Detection limits of 1.1 mg L^{-1}, 1.0 mg L^{-1}, 1.3 mg L^{-1} and 0.2 mg L^{-1} were obtained for As, Sb, Pb and Ge, respectively. Up to 77 times enhancement in detection limit of Pb were obtained, compared to the result obtained from the direct analysis of liquids by LIBS. Applicability of the technique to real water samples was tested through spiking experiments and recoveries higher than 80% were obtained. Results demonstrate that, HG-LIBS approach is suitable for quantitative analysis of toxic elements and sufficiently fast for real time continuous monitoring in aqueous environments.

1. Introduction

Laser-induced breakdown spectroscopy (LIBS) [1,2] is an optical emission spectroscopic technique that uses a powerful pulsed laser source to produce plasma on a variety of sample types: solids, liquids, gaseous and aerosols for a variety of applications: industrial, nuclear, geochemical, biomedical, military, space, planetary and environmental [3–11]. Time and space resolved analysis of characteristic atomic emission lines of the resultant plasma reveals information about the chemical content and the amount of the elements present. Some of the desirable properties like: its lack of need for sample preparation, multi-element capability, its speed and portability to the field make it extremely powerful analytical tool be used in environmental applications.

* Corresponding author. Tel.: +90 232 7507624; fax: +90 232 7507509.
E-mail address: serifeyalcin@iyte.edu.tr (Ş. Yalçın).

0003-2670/$ – see front matter © 2013 Elsevier B.V. All rights reserved.
http://dx.doi.org/10.1016/j.aca.2013.02.014

Applications of LIBS on direct analysis of liquids are not as many as the ones on solids due to splashing, bubble and shockwave evolution problems which give rise to poor signal quality, reduced plasma emission and high quantification limits. Some approaches to overcome difficulties encountered in bulk liquid analysis include plasma formation: on flowing-jet liquid [12,13], on the surface of the liquid [14,15], on single isolated droplets [16] and in cavitation bubbles [17]. Alternative to single-pulse LIBS experiments, double-pulse LIBS technique [18,19] has been successfully applied for the analysis of aqueous [20] and underwater [21] samples in which the first laser pulse is used to create a gaseous atmosphere and the second pulse produce plasma with reduced background emission and longer lifetimes. Therefore, double pulse LIBS approach presents higher sensitivity over single pulse LIBS experiments and the analytical capability of the technique increases.

Electrospray ionization [22,23] and proper nebulization techniques like pneumatic and ultrasonic nebulization also widely used to introduce liquid samples in the form of an aerosol [24,25]. Recently, analysis of liquids based on hydride generation sample introduction technique with laser-induced breakdown spectroscopic detection, HG-LIBS, for some of the hydride forming elements have been shown [27–29].

Hydride generation (HG) is a chemical derivatization process based on the formation of volatile hydrides from some of the elements of the periodic table in the presence of an acid and a strong reducing agent [26]. HG coupled with atomic spectrometric detection (HG-AAS, HG-ICP-OES, HG-AFS), is among the most common method for decades for its higher sensitivity and is widely used for quantification of As, Se, Bi, Ge, Sb, Sn, Te and Pb in liquid samples. However, there are a few studies based on coupling of the hydride generation system to laser-induced breakdown detection.

Singh et al. [27] have investigated the effect of the carrier gas (He, Ar) and pressure on LIBS spectra of stannane (SnH_4) and arsine (AsH_3) in a batch type hydride generation system. Experiments were performed in an evacuated chamber. Work does not contain any quantitative data on the sensitivity of the technique; however, a decrease in the analyte signal due to depletion of the hydrides in the closed system has been mentioned.

In our previous work [28], development of a hydride generation laser-induced breakdown spectroscopic technique, HG-LIBS, in continuous flow mode was realized. The chemical and instrumental parameters of the system were systematically studied in order to achieve optimal conditions for the determination of tin (Sn) in aqueous environments. Several orders of magnitude enhancement in signal intensity was observed in comparison to direct liquid analysis by LIBS with a detection limit of 0.3 mg L^{-1} for Sn.

A more recent study in literature on continuous flow HG-LIBS approach was performed by Simeonsson et al. [29], in which physical plasma parameters of arsine (AsH_3), stibine (SbH_3) and selenium hydride (H_2Se) plasma were evaluated in Ar only and Ar/H_2 gas mixture. Plasma electron density determined through hydrogen emission measurements was found to vary from 4.5×10^{17} to 8.3×10^{15} cm^{-3} over time delays of 0.2–15 μs. Plasma temperatures determined through argon and arsenic emission measurements range from 8800 to 7700 K for Ar and from 8800 to 6500 K for As in HG-LIBS plasmas. Little difference in the excitation temperatures was observed. However, a significant reduction in the intensity and lifetime of Ar atomic emission lines in the HG-LIBS plasmas that appeared to be due to the presence of H_2 was shown. Work does not include optimization of the chemical and instrumental LIBS parameters; however, limit of detection values of 0.7, 0.2 and 0.6 mg L^{-1}, were reported for arsenic, antimony and selenium, respectively. Results were obtained with a single wavelength detector, photomultiplier tube (PMT) and a boxcar averaging.

Here, in this paper a systematical analysis of chemical and instrumental parameters affecting HG-LIBS signal from arsine (AsH_3), stibine (SbH_3), plumbane (PbH_4) and germane (GeH_4) plasma is presented, for the first time. The effect of differing ambient gas, argon and nitrogen, on the sensitivity of the HG-LIBS signal has been studied. Strong enhancement in signal strength of arsenic, antimony and germanium were observed under argon atmosphere. In order to investigate the causes of the much higher line intensity in Ar observed for three of the elements, a deeper study was carried out. The plasma temperature and electron number density were determined for both gases as a function of detector delay time. Calibration graphs were constructed, and detection limits were evaluated. The applicability of HG-LIBS technique for the determination of As, Sb, Pb and Ge in aqueous environments was tested by spiking each element in real water samples. Quantitative analysis of aqueous samples by HG-LIBS method was evaluated.

2. Materials and methods

2.1. Experimental

The experimental set-up for continuous flow hydride generation LIBS system [28], consists of a hydride generation, plasma formation and detection units.

In the hydride generation part, the acidified analyte and $NaBH_4$ solutions are delivered to a three ways polytetrafluoroethylene (PTFE) connector (Supelco) by means of a four channel peristaltic pump (Longer Precision). U type gas–liquid separator (GLS) is used to separate gaseous hydrides from the solution. The drain of the waste solution is pumped from GLS with another peristaltic pump (ISMATEC, Germany). With a controlled flow of inert gas (Ar or N_2 flowing continuously), hydrides are carried through the Nafion membrane dryer unit (Permapure, MD50) in order to remove the moisture content. Volatile hydrides produced in the hydride generation unit are then passed to the five-armed Teflon sample/plasma cell from the top where they interact with laser pulses at an angle of 90° incidence with respect to incoming laser beam.

A Q-switched Nd:YAG laser (Spectra Physics, LAB 170-10) operating at the second harmonic (532 nm) wavelength with 10 ns pulse width and 10 Hz pulse repetition rate was used as a plasma source. The laser beam was focused by a 17.5 cm focal length plano-convex lens into the sample cell to form plasma from the gaseous hydrides. Plasma emission signal was collected and focused by using two 10.0 cm focal length plano-convex lenses onto the fiber optic cable (Ocean Optic, 600 μm). This fiber was then coupled to an echelle type spectrograph (ME5000, Andor Inc., f = 195 mm, 0.08 nm resolution), equipped with a gated, image intensified charge coupled detector, ICCD (iStar DH734, Andor Inc.). Wavelength calibration of the spectrograph was performed using a Hg–Ar lamp. Detector gain was kept at a setting of 100, and 10 shot accumulation spectra were used for most of the measurements.

2.2. Reagents

All reagents were of analytical grade or higher purity. Standard solutions of As, Sb, Pb and Ge were prepared daily from their 1000 mg L^{-1} stock solution (High-Purity Standards) through appropriate dilutions with ultra pure water. Sodium borohydride, $NaBH_4$ solutions were prepared by dissolving its powder (Sigma–Aldrich) in dilute NaOH (Riedel-de Haën) for stabilization and used without filtration. $NaBH_4$ solution was prepared in the presence of 1.0% (w/v) NaOH for antimony, 0.2% NaOH for arsenic and germanium, and 0.1% NaOH for lead. Otherwise stated, acidified standards/samples and reductant solutions were delivered to the GLS at a flow rate of 2.5 mL min^{-1} and 5.0 mL min^{-1}, respectively.

For antimony measurements, L-cysteine (Aldrich) was used as a pre-reducing agent and for lead, potassium hexacyanoferrate(III),

$K_3[Fe(CN)_6]$ (Sigma–Aldrich) was used as an oxidizing agent. In the presence of HCl and $K_3[Fe(CN)_6]$, a highly toxic product, "HCN", is formed, therefore, this substance should be handled extremely carefully. The HG system is a closed system and a fume hood placed at the top of the system was used to provide effective ventilation.

River Water Reference Material for trace metals, SLRS-4 (NRC, Ottowa, Canada), tap water (İzmir-Urla Municipal Water Supply) and bottled spring water (Pınar, Aydın, Turkey) were used without dilution. For recovery experiments, due to the presence of undetectable concentrations of the target elements (As, Sb, Pb, Ge), real water samples were spiked with known concentrations of a single element standards.

3. Results and discussion

In a HG-LIBS experiment, the type of the background/carrier gas and a number of instrumental and chemical variables need to be studied in order to maximize LIBS signal.

3.1. Effect of carrier gas type on HG-LIBS signal

The influence of the background gas on LIBS signal strength and the dynamics of the plasma plume expansion was vigorously studied in the past [29] and still is an active area in LIBS research. Experimental studies have shown that the nature and the pressure of background gas like Ar, He, Air, N_2, and CO_2 have significant effects on the physical plasma parameters, temperature and electron density, and on the analyte signal enhancement [27,30–34]. In this work, to investigate the effect of carrier gas type on HG-LIBS signal, continuous flow of argon and nitrogen gas was used to carry As, Sb, Pb and Ge hydrides from the gas-liquid separator into the plasma cell. Same analyte concentrations and identical instrumental and chemical conditions were used for recording a signal from the two different carrier gases.

Fig. 1(a)–(d) represents relative signal strength of each element under nitrogen and argon atmosphere. Solid lines represent signal in Ar and dotted lines represent signal in N_2 atmosphere.

As can be seen from the figure that, arsenic signal at 278.0 nm could only be observed under argon atmosphere, however lead signal at 405.8 nm, antimony signal at 259.8 and germanium signal at 265.1 nm were observed in the presence of both gases. Strong enhancement in Ge(I) and Sb(I) signal is observed under Ar atmosphere compared to nitrogen while Pb(I) signal intensity does not seem to be dependent on the type of the carrier gas. The same behavior was also observed for other emission lines of As(I), Sb(I) Pb(I) and Ge(I) within the full spectra. Therefore, optimization studies of arsenic, antimony and germanium were performed under argon environment while signal optimizations for lead were performed in the presence of nitrogen due to its lower cost.

Enhanced signal strength under Ar atmosphere is consistent with some literature work [35–37]. It has been reported that Ar gas provides higher signal intensity due to increased lifetime of Ar plasma and hence stable plasma temperatures and electron densities are obtained. The intensity enhancement of C and H lines in He plasma has also been reported by other groups [38,39]. In those studies, the enhancement mechanism due to the energy transfer from excited He or Ar atoms to the analyte atoms via Penning ionization was proposed.

In order to investigate the causes of the much higher line intensity observed in Ar atmosphere, electron density and temperature variation of HG-LIBS plasmas with respect to detector delay time were also evaluated. Plasma temperatures were determined from the Boltzmann equation [40] by using spectral emission intensities of neutral Ge(I) lines, based on the assumption that plasma is in

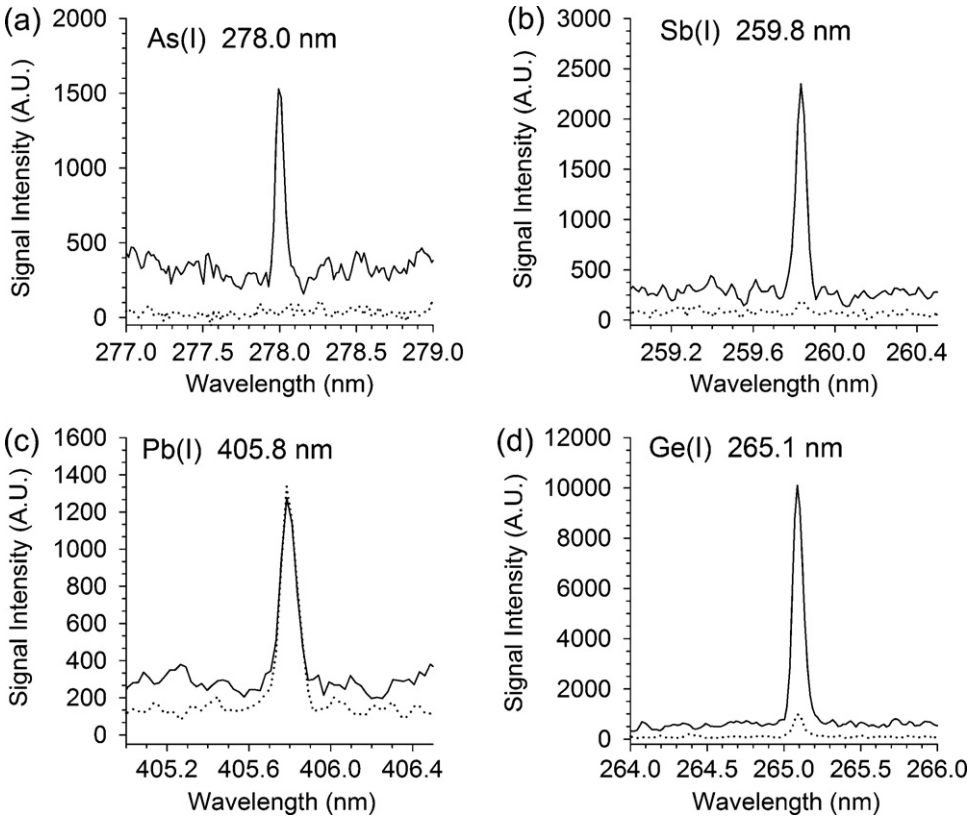

Fig. 1. Effect of carrier gas type on (a) As(I) 278.0 nm, (b) Sb(I) 259.8 nm, (c) Pb(I) 405.8 nm and (d) Ge(I) 265.1 nm emission line. Spectra recorded for 20.0 mg L^{-1} As, 40.0 mg L^{-1} Sb, 20.0 mg L^{-1} Pb and 20.0 mg L^{-1} Ge. Solid lines represent signal under Ar and dotted lines represent signal under N_2 atmosphere.

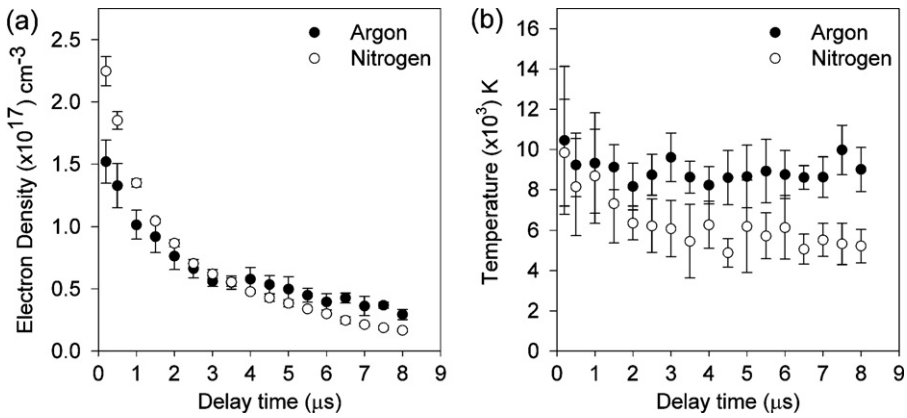

Fig. 2. Variation of (a) electron number density and (b) plasma temperature with respect to delay time. Neutral Ge(I) lines were used for temperature calculations (20.0 mg L^{-1} Ge in 1.0% HCl, 0.2% $NaBH_4$ in 0.2% NaOH, 126.0 mL min^{-1} Ar or N_2, t_g: 100 μs, LE: 100 mJ $pulse^{-1}$, $n = 7$).

local thermodynamic equilibrium (LTE). On the other hand, electron density values of the hydride plasmas were calculated from the Stark broadened profiles of neutral H(I) lines at 656.3 nm [40]. Fig. 2(a) and (b) shows the temporal variation of electron number density and plasma temperature in the presence of argon and nitrogen as carrier gases. Generally, electron number density decreases drastically as the detector delay time increases, from 1.5×10^{17} to 2.9×10^{16} for Ar and from 2.2×10^{17} to 1.6×10^{16} for N_2, due to ion-electron recombination processes. When the variation of plasma temperature in both argon and nitrogen atmosphere is considered, it has been found that Ar atmosphere has relatively higher temperatures than the ones in N_2 atmosphere, especially at late delay times. Between 0.2 μs and 8 μs time interval, plasma temperature that ranges from 10500 K to 8500 K in argon environment and 9832 K to 5216 K in N_2 environment were obtained. Also, the plasma temperature variation with respect to delay time in Ar is more stable than the one in N_2 atmosphere.

Results are consistent with the plasma temperatures presented by Simeonsson et al. through argon and arsenic line emission measurements [29]. The intensity enhancement in Ge emission lines, observed in this study, in the presence of Ar gas can be attributed to the Penning ionization process, in which, metastable states of Ar participate in the collision induced energy transfer process, as explained in the previous works by Sasaki et al. [37] and Lie et al. [39]. It may be proposed that; this secondary excitation of analyte atoms, Ge in this case, by metastable Ar atoms, in addition to initial laser pulse excitation, may lead to the state of sustained emission of analyte atoms in the HG-LIBS plasmas and hence the signal is enhanced.

3.2. Optimization of instrumental parameters

Laser type, laser wavelength, laser energy and detector timing parameters as delay and gate time are considered as some of the

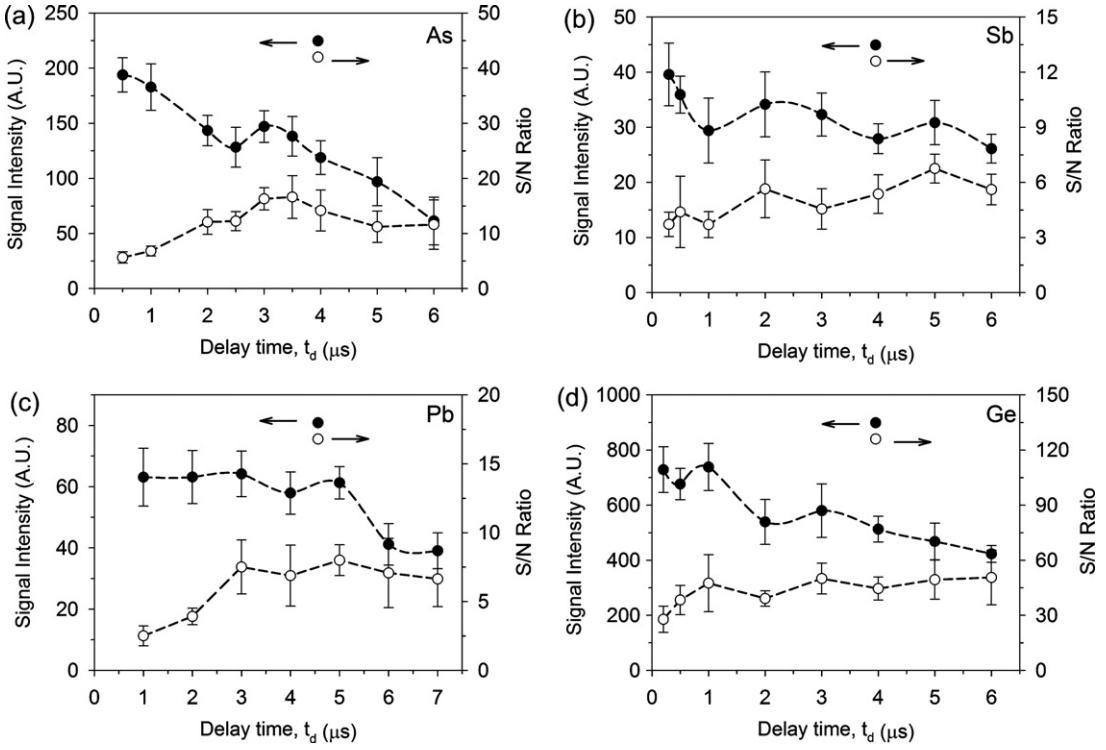

Fig. 3. Variation of LIBS signal intensity with respect to detector delay time, t_d, for (a) As(I) 278.0 nm, (b) Sb(I) 259.8 nm, (c) Pb(I) 405.8 nm and (d) Ge(I) 265.1 nm. Closed circles indicate relative signal intensity and open circles indicate S/N ratio. Spectra was recorded for 100.0 mg L^{-1} As, 100.0 mg L^{-1} Sb, 20.0 mg L^{-1} Pb and 20.0 mg L^{-1} Ge.

instrumental parameters in a LIBS experiment. In this study, the variation of LIBS signal strength with respect to laser pulse energy from a Nd:YAG laser at 532 nm, and detector timing parameters were studied.

3.2.1. Detector gating parameters and laser pulse energy

Time resolution experiments were performed for optimization of detector gating parameters such as delay time, t_d, and gate width, t_g.

In order to investigate the effect of delay time on LIBS signal variation, plasma emission signals from chemically generated hydrides were recorded at various detector delay times with respect to the laser pulse. Fig. 3(a)–(d) represents the variation of neutral As(I) 278.0 nm, Sb(I) 259.8 nm, Pb(I) 405.8 nm and Ge(I) 265.1 nm line intensity with respect to delay time.

In general, at early times of the plasma, relative signal intensity is higher and decreases as delay time increases. However, due to the presence of higher level of background at early delay times, the signal to noise ratio (S/N) consideration would be more accurate for the determination of optimal delay time. Therefore, the delay time at the maximum S/N was selected as optimum. The S/N data given in Fig. 3 were presented with empty circles and scaled on the right side of each graph, for every element under consideration. Here, signal is defined as the average of net peak height from 5 sequential measurements and the noise is defined as three times the standard deviation of the background in a region near the signal for the same number of measurements. Optimum t_d value for As, Sb, Pb and Ge was determined as 3.0 μs, 2.0 μs, 5 μs and 1 μs, respectively.

Variation of HG-LIBS signal with respect to detector gate width and laser pulse energy is given in Fig. 4(a) and (b), respectively. Here, compared to Sb, As and Pb signal, relatively higher signal strength is observed from the Ge lines, therefore, in order to show them all in the same figure, left axis was used for representing Ge line intensity while right axis was used for the other three elements. Similarly, the top axis of Fig. 4(a) corresponds to detector gating times for the element of arsenic. For arsenic, highest signal intensity was obtained with 750 μs gate width. Varying gating time from 10 μs to 50 μs resulted in a sharp increase in Sb signal however, beyond this value no noticeable change in signal intensity was observed. As seen from Fig. 4(a), gating time had no serious effect on Pb signal. In the case of germanium, changing gate width from 25 μs to 50 μs caused the signal to increase two times, while at 100 μs, a slight increase was observed. Thus, optimum gate widths were determined as 750 μs for arsenic, 50 μs for antimony and 100 μs for lead and germanium.

Laser pulse energy is another crucial instrumental variable needs to be optimized in laser induced plasmas. In order to determine optimum laser energy for LIBS measurements, plasma emission was recorded as a function of laser energy at optimum detector gating parameters. Data presented in Fig. 4(b) are for five replicate measurements and error bars on the graphs were obtained from the standard deviation of the signal. Generally, increasing laser pulse energy increases the emission intensity for all elements studied. After 100 mJ pulse^{-1} laser energy, deviation from the linearity that could be attributed to the plasma shielding effect was observed for As, Sb, and Ge.

3.2.2. Representative LIBS spectra under optimum experimental conditions

Representative LIBS spectra from arsine, stibine, plumbane, and germane plasma obtained under optimal instrumental and chemical conditions between 200 and 850 nm spectral interval are given in Fig. 5(a)–(d). For each element studied, several neutral atomic emission lines could be observed and insets of each figure detailed spectra representing the lines of interest is presented. In Fig. 5(a), neutral As(I) lines at 228.8 nm, 235.0 nm, 274.5 nm, 278.0 nm, and 286.0 nm are given. Representative spectrum from SbH_3 given in Fig. 5(b), shows four neutral emission lines of Sb(I) at 252.8 nm, 259.8 nm, 277.0 nm, and 287.8 nm. Three neutral emission lines of Pb(I) at 280.2 nm, 368.4 and 405.8 nm were given in Fig. 5(c). Besides, a well resolved sodium doublet emission at 589.0 and 589.6 nm and potassium doublet at 766.5 nm and 769.9 nm were also observed. Presence of these lines in spectra indicates Na and K transport from GLS to the Teflon plasma cell along with the gaseous hydrides. All spectra are strongly dominated by the neutral hydrogen line, H_α, at 656.3 nm which is produced from the dissociation of the metal hydrides under intense laser beam. Some argon emission lines in the far end of the visible region are also observed. Fig. 5(d) include seven neutral emission lines of germanium at 259.2 nm, 265.1 nm, 269.1 nm, 270.9 nm, 275.4 nm, 303.9 nm and 326.9 nm, which makes germanium a strong candidate to be used as a temperature sensor.

Quantitative measurements of As, Sb, Pb and Ge were performed at their most sensitive wavelengths of 278.0 nm, 259.8 nm, 405.8 nm and 265.1 nm, respectively.

3.3. Optimization of chemical parameters

It is well known that generation and transportation of volatile hydrides is very much dependent on various chemical parameters: such as acid and reductant concentration, presence of

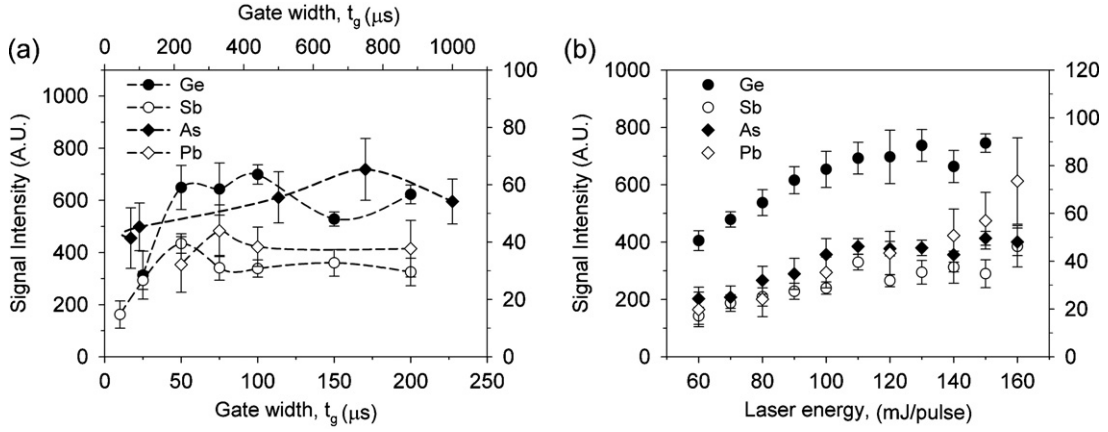

Fig. 4. Effect of (a) detector gate width, t_g, and (b) laser pulse energy on As(I) 278.0 nm, Sb(I) 259.8 nm, Pb(I) 405.8 nm and Ge(I) 265.1 nm signal. Spectra was recorded using 20.0 mg L^{-1} As, 100.0 mg L^{-1} Sb, 20.0 mg L^{-1} Pb and 20.0 mg L^{-1} Ge.

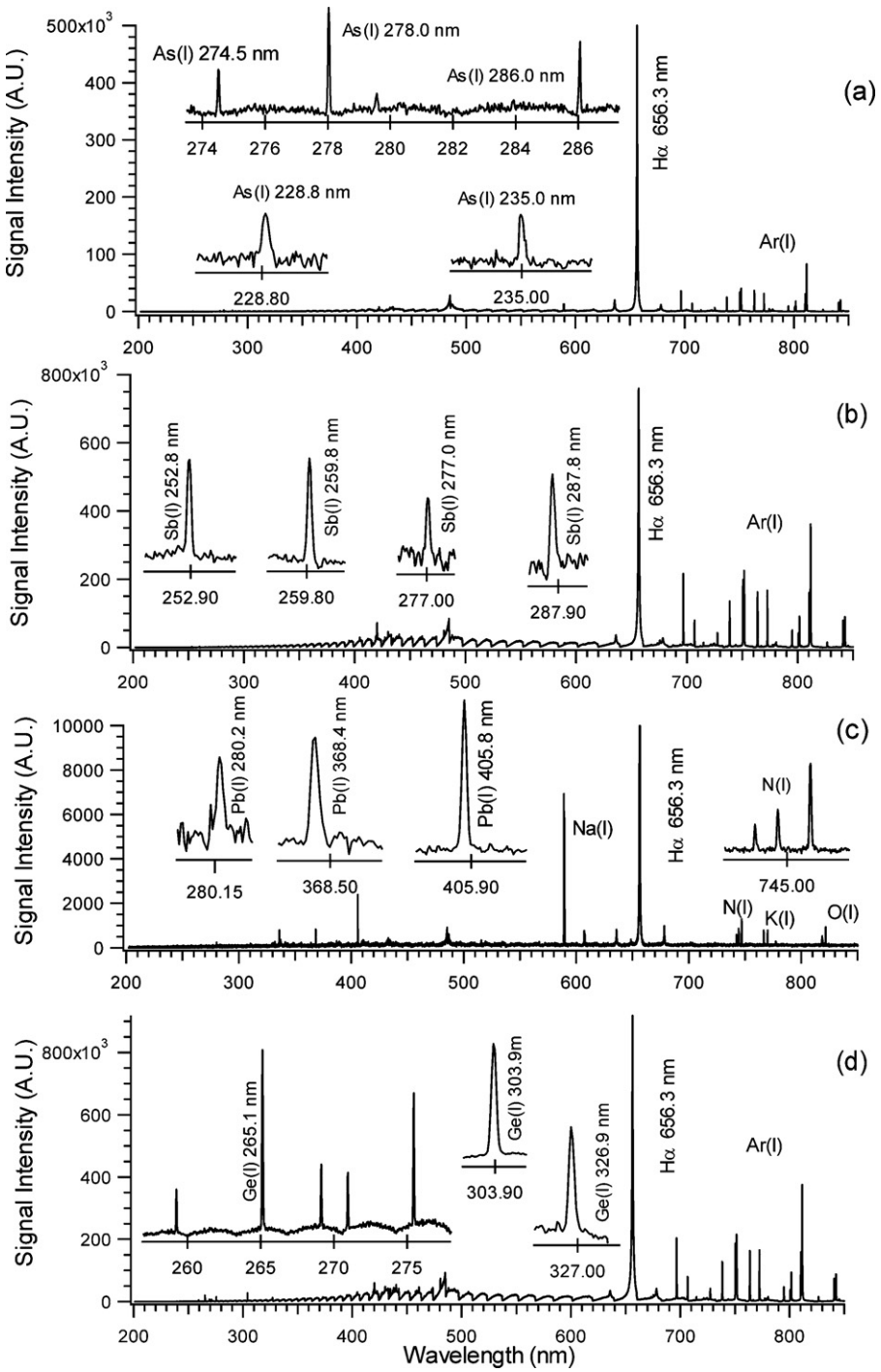

Fig. 5. Representative HG-LIBS spectra recorded from (a) arsine, (b) stibine, (c) plumbane and (d) germane plasma under optimum experimental conditions. Typical emission profiles of each element are presented inside each spectrum, in enlarged scale.

oxidizing/pre-reducing agent, sample and carrier gas flow rate. For this purpose, not only instrumental but also chemical parameters were also systematically investigated for each element to maximize HG-LIBS signal.

3.3.1. *Effect of pre-reducing agent,* L-*cysteine, on Sb HG-LIBS signal*

Oxidation of Sb(3+) to Sb(5+) might take place under acidic conditions, and pentavalent form of antimony presents significantly lower sensitivity than its trivalent form, during its detection from the chemically generated hydrides. L-Cysteine is known to have an effective pre-reduction capacity [41,42] and widely used in HG systems for reducing antimony into its lower oxidation state before detection.

In this study, due to low LIBS signal intensity obtained from Sb hydrides even with 100.0 mg L^{-1} Sb^{3+} solution concentrations, the effect of adding pre-reducing agent on LIBS signal strength was investigated. For this purpose Sb(I) signal at 259.8 nm were recorded in the presence of selected L-cysteine concentrations, between 0.2% and 5.0% (w/v), under optimum acid and reducing agent concentrations (2.0% HCl and 1.0% $NaBH_4$ in 1.0% NaOH). The effect of adding pre-reducing agent on LIBS signal strength of Sb(I)

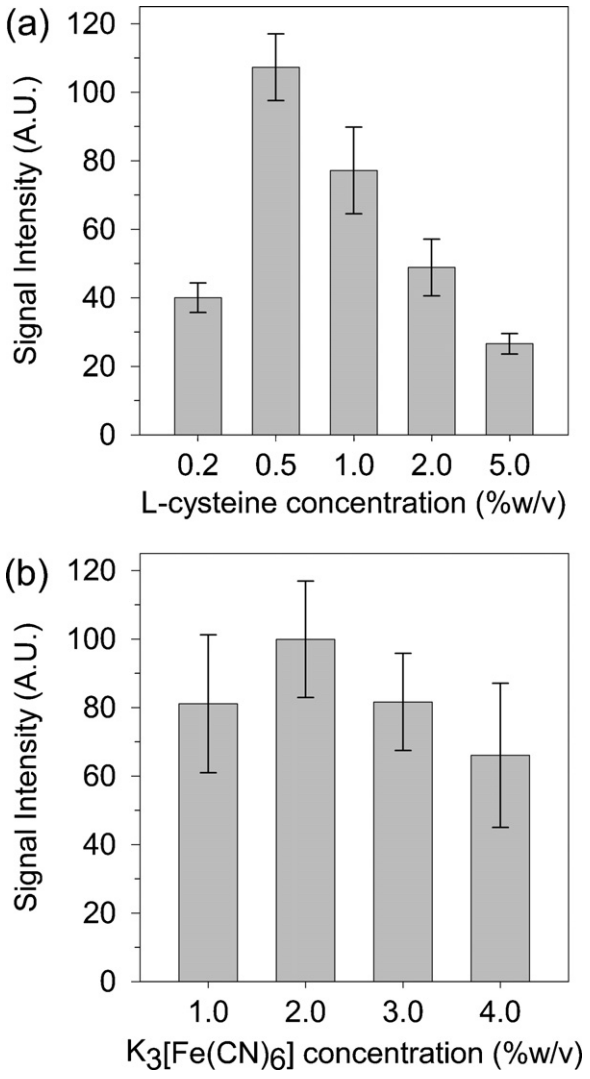

Fig. 6. (a) Variation in Sb(I) signal at 259.8 nm with respect to L-cysteine concentration. 100.0 mg L^{-1} Sb(+3) in 2.0% HCl, 1.0% $NaBH_4$ in 1.0% NaOH, t_d: 2 μs, t_g: 50 μs, carrier gas: 160 mL min^{-1} Ar, and laser energy: 100 mJ $pulse^{-1}$ were used. (b) Effect of oxidizing agent concentration on Pb(I) signal intensity at 405.8 nm. 100.0 mg L^{-1} Pb in 2.0% HCl, 1.0% $NaBH_4$ in 0.1% NaOH, t_d: 5 μs, t_g: 100 μs, carrier gas: 155 mL min^{-1} N_2, and LE: 150 mJ $pulse^{-1}$ were used.

is given in Fig. 6(a). More than two times enhancement in Sb(I) signal was obtained by increasing L-cysteine concentration from 0.2% to 0.5%. However, between 1.0% and 5.0% L-cysteine concentration, Sb signal started to decline, linearly. Therefore, optimum L-cysteine concentration was selected as 0.5% (w/v) and used accordingly for Sb analysis by keeping the rest of the parameters constant.

3.3.2. Effect of oxidizing agent, $K_3[Fe(CN)_6]$, on Pb HG-LIBS signal

Lead determination by hydride generation is known to be challenging due to the low yield and instability of plumbane. Several studies in the literature have shown that the reaction rate and signal sensitivity could be increased by the addition of an oxidizing agent: potassium hexacyanoferrate(III), $K_3[Fe(CN)_6]$ [43–45]. In order to increase the stability of lead hydrides, $K_3[Fe(CN)_6]$ was also used as an oxidizing agent in this study. Optimum oxidizing agent concentration was investigated by recording HG-LIBS signal from 20.0 mg L^{-1} Pb solutions in the presence of 1.0%, 2.0%, 3.0%, and 4.0% (w/v) potassium hexacyanoferrate(III). As is shown in Fig. 6(b), the highest Pb(I) signal at 405.8 nm was obtained when 2.0% $K_3[Fe(CN)_6]$ was used.

Another problem that has been faced during plumbane generation, due to a vigorous reaction between acid and $NaBH_4$, was the excessive foaming and aerosol carry over from GLS to membrane dryer. These foamy aerosols were adsorbed on the upper-inner walls of the GLS and inside the Teflon tubing that connects the GLS to membrane drying unit. This, in turn, reduced the reproducibility of the signal. In order to reduce aerosol carry over, data collection was performed while the carrier gas N_2 blowing above the liquid level instead of continuous bubbling inside.

3.3.3. Effect of acid concentration

The type and concentration of acid plays an essential role in hydride generation reactions. Various types of acids (such as hydrochloric acid, nitric acid, sulfuric acid, tartaric acid, acetic acid and hydrofluoric acid) may be used. Among these the most widely used one is HCl. In this study, analyte solutions were prepared in the range of 0.1–3.0% (v/v) HCl concentrations. Use of acid concentration higher than 5.0% (v/v) resulted in alteration in the plasma position due to production of excess hydrogen gas and could be recognized from the suppression of the analyte signal and the decrease in the powerful breakdown sound.

The effect of acid concentration on HG-LIBS signal strength for all four elements under study is presented in Fig. 7(a). Here, due to the higher signal intensity of Ge lines observed, compared to Sb, As and Pb signal, left axis of the figure was used for Ge line intensity while right axis was used for the representation of the rest. Each element behaves differently with changing acid concentrations. Neutral As(I) signal at 278.0 nm was not affected significantly by increasing acid concentration from 0.2% to 1.0% while after this concentration signal starts to decrease. Neutral Sb(I) LIBS signal at 259.8 nm, obtained from 40.0 mg L^{-1} Sb^{3+} in the presence of 0.5% L-cysteine solution, increases from 1.0% to 2.0% acid concentration and beyond this value the signal starts to decrease again. As it can be seen from the figure that neutral Pb(I) signal at 405.8 nm presents maximum sensitivity at 2.5% HCl concentration. Increasing HCl concentration from 0.2% to 1.0% results in a sharp increase in Ge(I) 265.1 nm signal and after this point, signal decreases drastically. Optimum acid concentrations for the analysis of As, Sb, Pb and Ge were selected as 1.0%, 2.0%, 2.5% and 1.0%, respectively, throughout the measurements. During acid optimization studies, $NaBH_4$ concentration was kept as 2.0% for arsenic and 1.0% for antimony, lead and germanium.

3.3.4. Effect of reductant, $NaBH_4$ concentration

Optimum $NaBH_4$ concentration was also investigated in order to achieve maximum response from arsenic, antimony, lead and germanium hydrides by HG-LIBS. Solutions prepared in differing $NaBH_4$ concentrations were reacted with analyte solutions prepared in dilute HCl. Resulting volatile hydrides purged with a flow of carrier gas and plasma emission signal were collected under optimum instrumental parameters. Signal strength variation with respect to $NaBH_4$ concentration for each element under consideration is given in Fig. 7(b). Left axis of the figure was used for Ge line intensity, and right axis was used for the representation of the Sb, As and Pb signal, due to relatively higher signal intensity of Ge lines.

Increasing $NaBH_4$ concentration from 0.05% to 0.5% increases arsenic signal two times. At higher concentrations signal decreases. Thus, 0.5% $NaBH_4$ was determined to be an optimal reductant concentration for arsenic. Sb(I) signal strength at 259.8 nm presents a sharp increase when $NaBH_4$ concentration was increased from 0.1% to 1.0%, then gradually decreases until 2.5% reductant concentrations. 1.0% $NaBH_4$ concentration was selected as an optimal reductant concentration for Sb.

Increasing reductant concentration from 0.5% to 1.0% increases Pb(I) signal at 405.8 nm and at higher concentrations signal

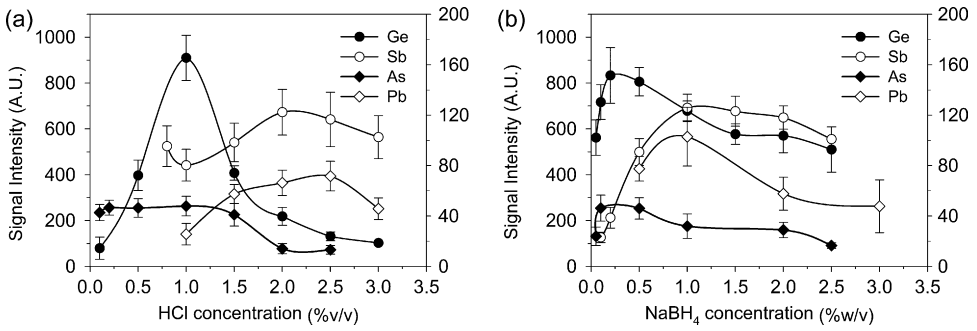

Fig. 7. (a)Variation of As(I) 278.0 nm, Sb(I) 259.8 nm, Pb(I) 405.8 nm and Ge(I) 265.1 nm LIBS signal intensity as a function of acid (HCl) concentration. During acid optimizations, $NaBH_4$ concentration of 2.0% for arsenic and 1.0% for antimony, lead and germanium were used. (b) The effect of reductant ($NaBH_4$) concentration on LIBS signal strength. Left axis of the figures was used for Ge line intensity, and right axis was used for the representation of the Sb, As and Pb signal.

decreases drastically and remains unchanged. Therefore, for lead determinations, optimum reductant concentration was selected as 1.0%. Similarly, optimal sodium borohydride concentration that can produce maximum Ge(I) signal at 265.1 nm was obtained at 0.2%.

3.3.5. Effect of sample flow rate

The acidified sample to the reductant flow rate was kept at a ratio of 1:2 by selecting an appropriate tubing size. Sample flow rate was adjusted to a desired flow rate by controlling pump rate. Three sample flow rate 1.0 mL min^{-1}, 2.5 mL min^{-1} and 4.0 mL min^{-1} were studied. Fig. 8(a) shows the effect of sample flow rate on As, Sb, Pb and Ge signal intensity. In order to present all elements on the same scale, Ge signal intensities were divided by ten.

Generally, increasing sample flow rate increases the signal strength, for each element studied, however, delivering the sample at a flow rate of 4.0 mL min^{-1} instead of 2.5 mL min^{-1} will result in condensation of arsine gas in the plasma cell and over consumption of sample and reagent. For Sb signal, no significant change was observed with the change in sample flow rate. Signal fluctuation remains within the range of error bars however; signal at 2.5 mL min^{-1} flow rate is slightly higher than 1.0 and 4.0 mL min^{-1} flow rates. Similarly, for both Pb and Ge, maximum analyte response was observed at 2.5 mL min^{-1} sample flow rate. Therefore, 2.5 mL min^{-1} sample flow rate was selected as optimum for all elements studied.

3.3.6. Carrier gas flow rate

Although they are volatile, fast and efficient transport of hydrides from the reaction medium to the sample cell is necessary for obtaining highly sensitive measurements. Both, the type and the flow rate of the carrier gas have a significant influence on the signal strength. As discussed in Section 3.1, transportation of arsine, stibine and germane from GLS to sample/plasma cell was performed by using argon gas and for plumbane nitrogen gas was used. In order to study the effect of carrier gas flow rate, analyte signal from each element at their maximum emission wavelength was recorded as a function of carrier gas flow rates. The effect of carrier gas flow rate on As, Sb, Pb and Ge signal strength is shown in Fig. 8(b). Maximum sensitivities were obtained at 126 mL min^{-1}, 160 mL min^{-1} and 126 mL min^{-1} Ar flow rates for As, Sb and Ge, respectively. For Pb(I), maximum signal was obtained at 155 mL min^{-1} flow rate of N_2. Table 1 lists optimum conditions for all instrumental and chemical parameters studied.

3.4. Calibration graphs and detection limits

In order to determine the applicability of the HG-LIBS technique for quantitative analysis of As, Sb, Pb and Ge present in aqueous environments, calibration graphs were constructed, and detection limits were determined. Under optimal experimental and chemical conditions listed in Table 1, LIBS plasma emission from different analyte concentrations of a single element standards were used to

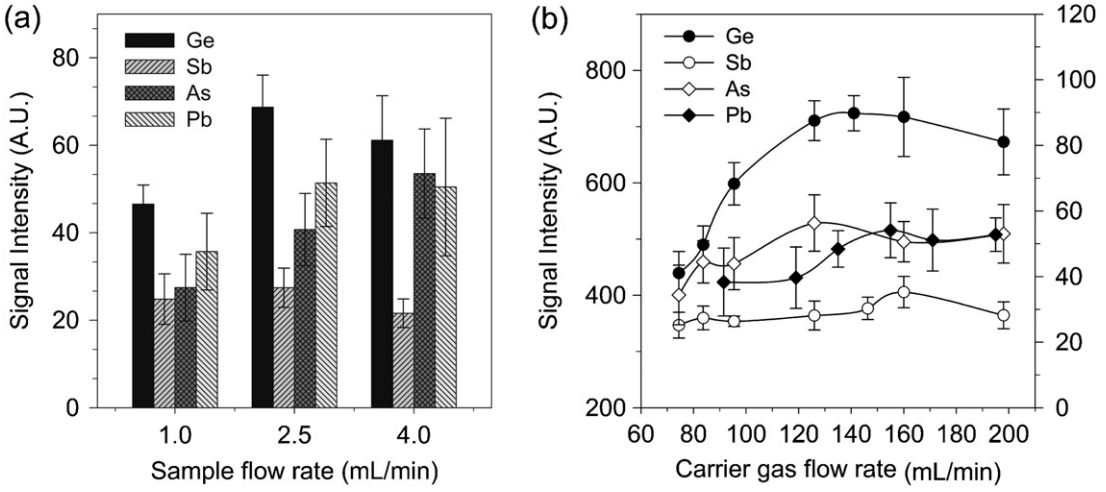

Fig. 8. Effect of (a) sample flow rate and (b) carrier gas flow rate on As(I) 278.0 nm, Sb(I) 259.8 nm, Pb(I) 405.8 nm and Ge(I) 265.1 nm signal intensity, under optimum instrumental and chemical conditions of the HG-LIBS system.

Table 1
Optimum instrumental and chemical conditions of HG-LIBS system and LOD values for As, Sb, Pb and Ge analysis.

	As	Sb	Pb	Ge
Spectral line (nm)	278.0	259.8	405.8	265.1
Laser energy (mJ pulse^{-1})	130	160	150	130
t_d (μs)	3	2	5	1
t_g (μs)	750	50	100	100
$NaBH_4$ conc. (w/v, %)	0.5	1.0	1.0	0.2
$NaBH_4$ flow rate (mL min^{-1})	5.0	5.0	5.0	5.0
HCl conc. (v/v, %)	1.0	2.0	2.5	1.0
Sample flow rate (mL min^{-1})	2.5	2.5	2.5	2.5
Pre-reducing/oxidizing agent conc. (w/v, %)	–	0.5[a]	2.0[b]	–
Carrier gas flow rate (mL min^{-1})	126	160	155	126
Limit of detection (mg L^{-1})	1.1	1.0	1.3	0.2

[a] L-Cysteine was used as a pre-reducing agent.
[b] $K_3[Fe(CN)_6]$ was used as an oxidizing agent.

produce calibration graphs and are shown in Fig. 9(a)–(d). Measurements were performed at the most sensitive atomic emission lines of As (278.0 nm), Sb (259.8 nm), Pb (405.8 nm) and Ge (265.1 nm). Data points in graphs represent average of 10 replicate measurements each from the accumulation of 10 single laser shots and error bars are from the standard deviations of those measurements. As can be seen from the figure that, As, Sb and Pb signal exhibit linear response with respect to analyte concentration and linear regression constants, R^2, are close to 0.99 for all. In the case of germanium, Fig. 9(d), the plot shows a deviation from linearity after 20.0 mg L^{-1} Ge concentration and regression constant value drops from 0.9978 to 0.9770 when the concentration range is extended to 50.0 mg L^{-1}, indicating a loss of sensitivity at high concentrations. This loss of sensitivity and hence deviation from linearity at high concentrations can be explained by self-absorption of resonance transition lines. In LIBS plasmas, self-absorption of the resonance lines is highly anticipated.

Detection limits calculated from the slopes of the calibration curves were based on 3σ criterion, where σ is the standard deviation of the background and LOD values of 1.1 mg L^{-1}, 1.0 mg L^{-1}, 1.3 mg L^{-1} and 0.2 mg L^{-1} were obtained for As, Sb, Pb and Ge, respectively.

Detection limits obtained for As, and Sb in this study are comparable with the ones in literature [26,28] obtained by HG-LIBS method. A detection limit of 1.0 mg L^{-1} for As is reported by Singh et al., and LOD values of 0.7 mg L^{-1} for arsenic and 0.2 mg L^{-1} for antimony were reported by Simeonsson et al. Both results do not include optimization studies and are based on PMT type detection that could provide higher quantum efficiencies at the wavelengths of interest and larger detection area compared to ICCD type detectors.

To the best of our knowledge, there is no record in the literature based on HG-LIBS detection of Pb and Ge, however, there are several reports on the determination of Pb in aqueous solutions based on direct liquids analysis by LIBS. Detection limits of 40 mg L^{-1} [6], and 100 mg L^{-1} Pb [14] were reported for experiments on liquid-jet and in bulk water analysis, respectively. In our previous work [25], a detection limit of 13.6 mg L^{-1} Pb was obtained from a LIBS system that utilize an ultrasonic nebulizer to produce sub-micron size aerosols. An LOD value of 1.3 mg L^{-1} Pb obtained in this study by the HG-LIBS technique, presents 10 times enhancement compared to that of by ultrasonic nebulization sample introduction system. Result also shows 30 and 77 times enhancement in LOD values compared to direct analysis of liquid samples by LIBS on liquid-jet and

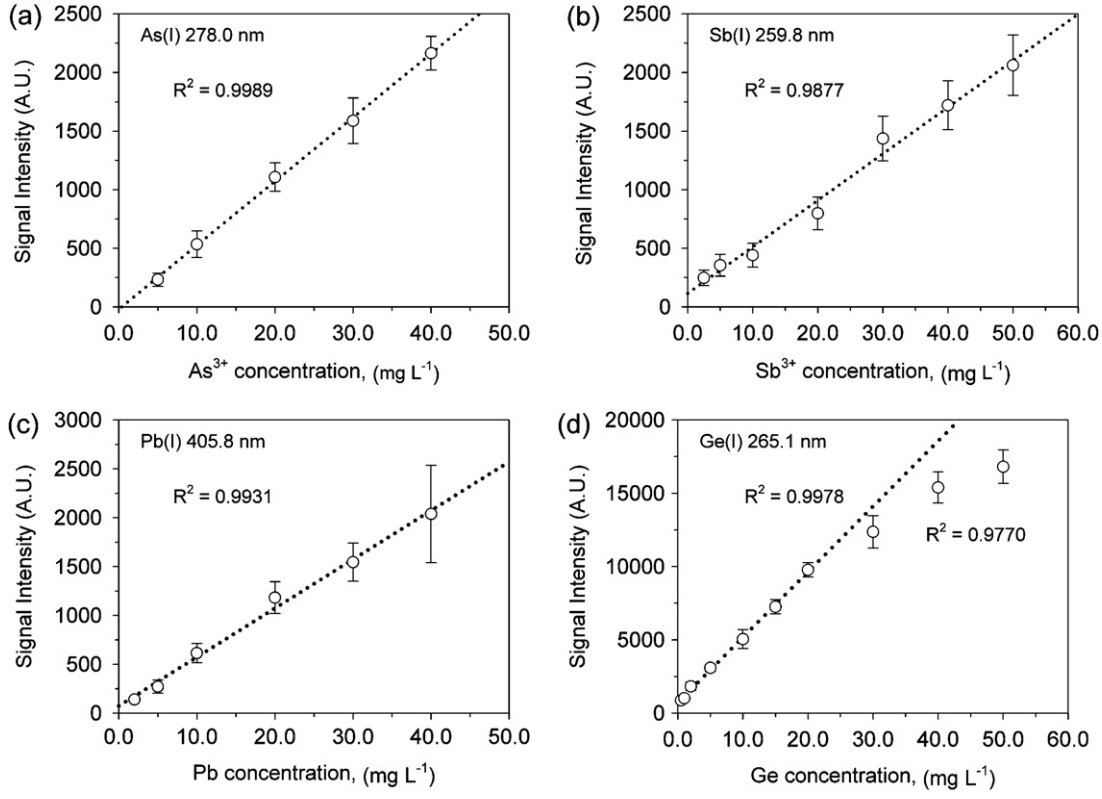

Fig. 9. Calibration graphs for (a) As(I) 278.0 nm, (b) Sb(I) 259.8 nm, (c) Pb(I) 405.8 nm and (d) Ge(I) 265.1 nm emission lines under optimum experimental and chemical conditions. Each datum represents average of 10 replicate measurements, each from the accumulation of 10 single laser shots and error bars are from the standard deviations of those measurements.

Table 2
Recovery results from the real water samples spiked with a single element standard solutions.

	% recovery ± SD			
	As	Sb	Pb	Ge
River water, SLRS-4	80.9 ± 12.9	98.3 ± 14.6	128.9 ± 18.9	100.3 ± 9.5
Tap water, Urla municipal water	84.2 ± 4.0	98.9 ± 15.3	129.7 ± 11.1	90.5 ± 13.5
Drinking water, spring water, Aydın	100.9 ± 19.4	100.1 ± 10.8	108.9 ± 15.6	123.9 ± 7.8

No detectable As, Sb, Pb and Ge signal before spiking by HG-LIBS system. 5 mg L^{-1} Ge and 10 mg L^{-1} As, Sb and Pb were used for spiking real water samples.

in bulk water, respectively. Results are promising in terms of the applicability of the HG-LIBS technique to quantitative analysis of toxic elements.

3.5. Application to real water samples

In order to validate HG-LIBS method for quantitative analysis of As, Sb, Pb and Ge in environmental water samples, River Water Reference Material for trace metals, SLRS-4, tap water from the local laboratory and drinking water provided from a local market, were analyzed for As, Sb, Pb, and Ge content. The concentrations of elements present in real water samples are at μg L^{-1} (ppb) level, which are below the detection limit of the HG-LIBS method. Therefore, water samples were ingested (spiked) with single standard solutions of 5 mg L^{-1} concentration for Ge and 10 mg L^{-1} concentration for As, Sb and Pb to achieve desired final concentration. Then, the analyte content was determined under optimum chemical and experimental conditions, and recoveries were calculated.

Percent recovery results obtained from the average of 10 replicate measurements are given in Table 2. In general, for all types of water samples, recovery values within ±20% standard deviation were obtained. Sb was among the best, with recoveries higher than 98%. Arsenic presents recoveries higher than 80% for all water samples studied. For lead, higher than 100% recoveries obtained for all types of water samples could be due to non-equilibrated reaction medium from the addition of $K_3[Fe(CN)_6]$, since standards and samples were prepared at the same time and the calibration standards were analyzed prior to the samples. Therefore, samples have more time for the reaction to be completed. Germanium has shown recoveries of 100.3% and 90.5% and 123.9% for river, tap and drinking water, respectively.

The precision of laser-induced plasma measurements depends largely on shot to shot reproducibility of the laser pulses, however, homogeneity and complexity of the sample has also considerable influence on the formation and evolution of the plasma and its dynamics. LIBS technique usually has low precision and accuracy with a typical RSD value in the range of 5–10%. Relatively worse precision values obtained from this work could be attributed to inhomogeneity of the plasma and possible matrix effect through chemical hydride generation process, which could be a subject to a more detailed study. Further investigations on the interference effect from the presence of other hydride forming elements will provide additional insights into the applicability of the HG-LIBS technique for the routine analysis of toxic elements in aqueous samples.

4. Conclusion

A systematic study on optimization of instrumental and chemical parameters of a HG-LIBS system was performed for the first time, in an attempt to analyze arsenic, antimony, lead and germanium in environmental water samples. Results showed that, HG-LIBS signal is significantly affected by the type of the ambient gas. Strong enhancement observed in argon atmosphere for As, Sb and Ge lines may be attributed to the Penning ionization effect in which metastable Ar atoms contribute to the establishment of a state of sustained emission of analyte atoms in HG-LIBS plasmas.

HG-LIBS technique described here is applicable to the direct and continuous analysis of water samples at low mg L^{-1} concentrations. Under optimum experimental conditions, detection limits of 1.1 mg L^{-1} for As, 1.0 mg L^{-1} for Sb, 1.3 mg L^{-1} for Pb and 0.2 mg L^{-1} for Ge were obtained. Detection limits obtained in this study are still higher than other conventional atomic spectrometric techniques (AAS, ICP-OES), that utilize hydride generation sample introduction method, however, entirely different atomization and excitation dynamics of laser-produced plasmas make a direct comparison of the analytical figures of merits difficult.

In this study, HG-LIBS technique has shown up to 77 times improvement in LOD for Pb, compared to literature value obtained by direct LIBS analysis of bulk liquid samples. Further enhancements may be achieved by using double-pulse LIBS technique.

HG-LIBS technique has been applied to the analysis of real water samples from spiking experiments, and recovery values higher than 80% were obtained for all types of water samples. Considering some inherent advantages of the LIBS technique, like its speed, ability to identify all elements in situ, with a single laser pulse, the proposed approach can be useful for the development of a portable LIBS sensor for the diagnosis and monitoring of environmental pollutants.

Acknowledgments

The authors thank the İzmir Institute of Technology, IYTE and the Scientific and Technological Research Council of Turkey, TÜBİTAK, for their financial support through research projects: BAP-12 and 109T327.

References

[1] L.J. Radziemski, D.A. Cremers, Laser-Induced Plasmas and Applications, Marcel Dekker, New York, 1989.
[2] A.W. Miziolek, V. Palleschi, I. Schechter (Eds.), Laser-Induced Breakdown Spectroscopy: Fundamentals and Applications, Cambridge University Press, New York, 2006.
[3] C. Lopez-Moreno, S. Palanco, J.J. Laserna, F. DeLucia Jr., A.W. Miziolek, J. Rose, R.A. Walters, A.I. Whitehouse, J. Anal. At. Spectrom. 21 (2006) 55–60.
[4] L. St-Onge, M. Sabsabi, P. Cielo, Spectrochim. Acta B 53 (1998) 407–415.
[5] R.J. Lasheras, C. Bello-Gálvez, E.M. Rodríguez-Celis, J. Anzano, J. Hazard. Mater. 192 (2011) 704–713.
[6] O. Samek, D.C.S. Beddows, J. Kaiser, S.V. Kukhlevsky, M. Liška, H.H. Telle, J. Young, Opt. Eng. 39 (2000) 2248.
[7] S. Koch, W. Garen, M. Müller, W. Neu, Appl. Phys. A: Mater. 79 (2004) 1071–1073.
[8] E. Cheng, R. Fraser, J. Eden, Appl. Spectrosc. 45 (1991) 949–952.
[9] L. Dudragne Ph., A.J. Amouroux, Appl. Spectrosc. 52 (1998) 1321–1327.
[10] E.M. Cahoon, J.R. Almirall, Anal. Chem. 84 (2012) 2239–2244.
[11] M.E. Asgill, D.W. Hahn, Spectrochim. Acta B 64 (2009) 1153–1158.
[12] N.K. Rai, A. Rai, J. Hazard. Mater. 150 (2008) 835–838.
[13] S.L. Lui, Y. Godwal, M.T. Taschuk, Y.Y. Tsui, R. Fedosejevs, Anal. Chem. 80 (2008) 1995–2000.
[14] P. Fichet, P. Mauchien, J.F. Wagner, C. Moulin, Anal. Chim. Acta 429 (2001) 269–278.
[15] J. Gruber, J. Heitz, H. Strasser, D. Bäuerle, N. Ramaseder, Spectrochim. Acta B 56 (2001) 685–693.
[16] S. Groh, P.K. Diwakar, C.C. Garcia, A. Murtazin, D.W. Hahn, K. Niemax, Anal. Chem. 82 (2010) 2568–2573.
[17] S. Koch, R. Court, W. Garen, W. Neu, R. Reuter, Spectrochim. Acta B 60 (2005) 1230–1235.
[18] V.S. Burakov, N.V. Tarasenko, M.I. Nedelko, V.A. Kononov, N.N. Vasilev, S.N. Isakov, Spectrochim. Acta B 64 (2009) 141–146.

[19] J.L. Gottfried, F.C. De Lucia Jr., C.A. Munson, A.W. Miziolek, Spectrochim. Acta B 62 (2007) 1405–1411.
[20] K. Rifai, S. Laville, F. Vidal, M. Sabsabi, M. Chaker, J. Anal. At. Spectrom. 27 (2012) 276–283.
[21] A. De Giacomo, M. Dell'Aglio, F. Colao, R. Fantoni, V. Lazic, Appl. Surf. Sci. 247 (2005) 157–162.
[22] J.-S. Huang, H.-T. Liu, K.-C. Lin, Anal. Chim. Acta 581 (2007) 303–308.
[23] J.S. Huang, K.C. Lin, J. Anal. At. Spectrom. 20 (2005) 53–59.
[24] P. Diwakar, P. Jackson, D. Hahn, Spectrochim. Acta B 62 (2007) 1466–1474.
[25] N. Aras, S. Ünal Yeşiller, D. Arıca Ateş, S. Yalcin, Spectrochim. Acta B 74–75 (2012) 87–94.
[26] J. Dedina, D. Tsalev, Hydride Generation Atomic Absorption Spectrometry, Wiley and Sons, New York, 1995.
[27] J.P. Singh, H. Zhang, F.Y. Yueh, K.P. Carney, Appl. Spectrosc. 50 (1996) 764–773.
[28] S. Ünal, S. Yalçın, Spectrochim. Acta B 65 (2010) 750–757.
[29] J. Simeonsson, L. Williamson, Spectrochim. Acta B 66 (2011) 754–760.
[30] F. Garrelie, C. Champeaux, A. Catherinot, Appl. Phys. A 69 (Suppl.) (1999) S55–S58.
[31] J.A. Aguilera, C. Aragon, Appl. Phys. A 69 (Suppl.) (1999) S475–S478.
[32] B. Salle, D.A. Cremers, S. Maurice, R.C. Wiens, Spectrochim. Acta B 60 (2005) 479–490.
[33] K. Kagawa, M. Ohtani, S. Yokoi, S. Nakajima, Spectrochim. Acta B 39 (1984) 525–536.
[34] S.S. Bindhu, Harilal C.V., V.P.N. Nampoori, C.P.G. Vallabhan, Appl. Phys. Lett. 72 (2) (1998) 167–169.
[35] Y. Lida, Appl. Spectrosc. 43 (1989) 229–234.
[36] Y. Lida, Spectrochim. Acta B 45 (1990) 1353–1367.
[37] Y. Sasaki, K. Wagatsuma, Anal. Sci. 25 (2009) 481–485.
[38] C.A. Henry, P.K. Diwakar, D.W. Hahn, Spectrochim. Acta B 62 (2007) 1390–1398.
[39] Z.S. Lie, H. Niki, K. Kagawa, May On Tjia, R. Hedwig, M. Pardede, E. Jobiliong, M.M. Suliyanti, S.N. Abdulmadjid, K.H. Kurniawan, J. Appl. Phys. 109 (2011) 103305.
[40] H.R. Griem, Plasma Spectroscopy, McGraw-Hill, New York, 1964.
[41] B. Welz, M. Sucmanova, Analyst 118 (1993) 1417–1423.
[42] A. D'Ulivo, L. Lampugnani, G. Pellegrini, R. Zamboni, J. Anal. At. Spectrom. 10 (1995) 969–974.
[43] A. D'Ulivo, M. Onor, R. Spiniello, E. Pitzalis, Spectrochim. Acta B 63 (2008) 835–842.
[44] J. Tyson, R. Ellis, G. Carnrick, F. Fernandez, Talanta 52 (2000) 403–410.
[45] I.D. Brindle, R. McLaughlin, N. Tangtreamjitmun, Spectrochim. Acta B 53 (1998) 1121–1129.